Published in final edited form as:
IEEE J Transl Eng Health Med. 2013 October 16; 1: . doi:10.1109/JTEHM.2013.2285916.

Novel Flurometric Tool to Assess Mitochondrial Redox State of Isolated Perfused Rat Lungs after Exposure to Hyperoxia

R. Sepehr, **S. H. Audi**[‡], **K. S. Staniszewski**, **S. T. Haworth**, **E. R. Jacobs**, and **M. Ranji**[‡]

Abstract

Recently we demonstrated the utility of optical fluorometry to detect a change in the redox status of mitochondrial autofluorescent coenzymes NADH (Nicotinamide Adenine Dinucleotide) and FAD (oxidized form of Flavin Adenine Dinucleotide (FADH2,)) as a measure of mitochondrial function in isolated perfused rat lungs (IPL). The objective of this study was to utilize optical fluorometry to evaluate the effect of rat exposure to hyperoxia (>95% O2 for 48 hours) on lung tissue mitochondrial redox status of NADH and FAD in a nondestructive manner in IPL. Surface NADH and FAD signals were measured before and after lung perfusion with perfusate containing rotenone (ROT, complex I inhibitor), potassium cyanide (KCN, complex IV inhibitor), and/or pentachlorophenol (PCP, uncoupler). ROT- or KCN-induced increase in NADH signal is considered a measure of complex I activity, and KCN-induced decrease in FAD signal is considered a measure of complex II activity. The results show that hyperoxia decreased complex I and II activities by 63% and 55%, respectively, as compared to lungs of rats exposed to room air (normoxic rats). Mitochondrial complex I and II activities in lung homogenates were also lower (77% and 63%, respectively) for hyperoxic than for normoxic lungs. These results suggest that the mitochondrial matrix is more reduced in hyperoxic lungs than in normoxic lungs, and demonstrate the ability of optical fluorometry to detect a change in mitochondrial redox state of hyperoxic lungs prior to histological changes characteristic of hyperoxia.

Index Terms

NADH dehydrogenase (complex I); succinate dehydrogenase (complex II); Flavin Adenine Dinucleotide ($FADH_2$); Nicotinamide Adenine Dinucleotide (NADH); lung surface fluorometry; mitochondrial redox

I. Introduction

High oxygen (O_2) therapy (hyperoxia) is a necessary treatment of low blood O_2 in adult and pediatric patients with acute lung injury (ALI) [1–3]. This treatment is effective in restoring blood pO_2 to a level which sustains vital organ metabolic requirements. However, prolonged exposure to high O_2 concentrations (>50%) causes lung injury [3–7]. Further complicating this situation is the fact that the time frame over which hyperoxic lung injury develops is difficult to predict due to the wide variation between patient tolerance/susceptibility [8].

Correspondence to: M. Ranji.
[‡]Co-Senior authors

Thus, a minimally invasive method to detect pulmonary injury in an individual patient exposed to high fractions of O_2 in real time is highly desirable.

Rat exposure to > 95% O_2 is a well-documented model of hyperoxic lung injury and human ALI [5, 8–10]. Previous studies have suggested that mitochondrial dysfunction is a cardinal feature of hyperoxic lung injury [11–16]. Although much work has been done in cell cultures and tissue homogenates, studies probing key tissue mitochondrial functions and the effect of oxidant injury in intact lungs in real-time are limited [11, 12, 17]. Because indices of mitochondrial function of *in situ* tissue are often different than those of tissue homogenates, measurements of indices of oxidative phosphorylation in intact tissue for comparison to those of isolated mitochondria are important.

Recently, we demonstrated the utility of optical fluorometry (Fig. 1) to detect a change in the redox status of lung mitochondrial autofluorescent coenzymes NADH (Nicotinamide Adenine Dinucleotide) and FAD (oxidized form of Flavin Adenine Dinucleotide ($FADH_2$,)) in isolated perfused rat lungs [18]. NADH and $FADH_2$ (Flavin Adenine Dinucleotide) are mitochondrial metabolic coenzymes, and are the primary electron carriers in oxidative phosphorylation. The oxidation of these two via the mitochondrial electron transport chain involves the transport of protons from mitochondrial complexes I, III, and IV into the mitochondrial intermembrane space (Fig. 2). This creates a proton gradient, which, along with the presence of adenosine diphosphate (ADP), yields the production of the cell's basic unit of energy, adenosine triphosphate (ATP). This process accounts for approximately 85% of ATP production in lung tissue [19]. Therefore, a change in the redox state of the electron transport chain, and thus NADH and $FADH_2$, is a quantitative marker of lung tissue mitochondrial bioenergetics, and hence mitochondrial function [10, 20].

The objective of this study was to utilize optical fluorometry to evaluate the effect of rat exposure to hyperoxia (>95% O_2 for 48 hours) on lung tissue mitochondrial redox status in a nondestructive manner in intact lungs, with a long term goal of understanding the role of mitochondrial dysfunction in the pathogenesis of lung O_2 toxicity as well as developing a diagnostic modality of oxygen toxicity.

II. Materials and methods

A. Materials

Fatty-acid free bovine serum albumin (Standard Powder, BSA) was purchased from Serologicals Corp. (Gaithersburg, MD). All other reagent grade chemicals were purchased from Sigma Chemical Company.

B. Fluorometer

A schematic for the fluorometer device used in these studies is shown in Fig. 1. The operation of this device has been described previously [18]. Briefly, excitation light is generated from a mercury arc lamp and delivered through a liquid light guide to a filter wheel, where the appropriate excitation wavelength can be selected. On the other side of this filter wheel is one leg of a bifurcated fiber bundle with a distal end of 3.2 mm inner diameter consisting of 158 (79 for excitation and 79 for emission) randomly distributed fibers, each

200 μm in diameter, which is brought into contact with the tissue, with minimal pressure on the lung. the power of the light emitted from the head of the probe is 1 mW/cm^2 for NADH and 4 mW/cm^2 for FAD. The other leg of the bifurcated fiber bundle delivers light to the detection optics where it is collimated and split using a beam splitter. Half of the light is then incident on an avalanche photodiode for detection of reflected light. The other half of the light then passes through a dichroic mirror to separate the NADH and FAD channels. In either of the channels, the light is then filtered to select the emitted fluorescence and is finally incident on a photomultiplier tube. To optimally excite the fluorophores of interest, NADH and FAD, using the mercury arc lamp, the excitation filters used were centered at 370 nm and 452 nm, with bandwidths of 40 nm and 50 nm, respectively. Finally, the filters used to detect the emitted fluorescence are centered at 460 and 520 nm, respectively, each with a bandwidth of 40 nm.

C. Animals

For normoxic (control) lung studies, adult male Sprague-Dawley rats (Charles River; 300–350 g) were exposed to room air. For the hyperoxic lung studies, age matched rats were housed in a Plexiglass chamber maintained at >95% O_2 for 48 hours (hyperoxic) [21]. The total gas flow was 3.5 liters/min and the chamber CO_2 was maintained at < 0.5%. The temperature within the chamber was 20–22°C. Every other day, the rats were weighed, and their cage, food, water, and CO_2 absorbent were changed. All rats were kept on a 12:12-h light-dark cycle. A total of 17 normoxic and 16 hyperoxic rats were studied. All animal experiments were performed under the approval of Institutional Animal Care and Use Committees of the Zablocki Veterans Affairs Medical Center and Marquette University (Milwaukee, WI) and in compliance with the National Research Council's Guide for the Care and Use of Laboratory Animals. For the hyperoxic rats, the optical imaging and other studies described below were conducted immediately following the exposure period.

D. Isolated perfused rat lung preparation

The isolated perfused lung preparation allows for manipulation of lung tissue mitochondrial redox state without disrupting the multi-cellular environment of the lung through the addition of metabolic inhibitor(s) to the recirculating perfusate and/or alteration of the composition of the ventilation gas [18].

As previously described, rats were anesthetized with pentobarbital sodium (40 mg/kg body wt. i.p.), the chest opened and heparin (0.7 IU/g body wt.) injected into the right ventricle [18]. The pulmonary artery and the trachea were cannulated, and the pulmonary venous outflow was accessed via a cannula in the left atrium. The heart-lung was removed from the chest and attached to a ventilation and perfusion system. The control perfusate contained (in mM) 4.7 KCl, 2.51 $CaCl_2$, 1.19 $MgSO_4$, 2.5 KH_2PO_4, 118 NaCl, 25 $NaHCO_3$, 5.5 glucose, and 3% fatty-acid free bovine serum albumin (BSA) [22]. The perfusion system was primed (Masterflex roller pump) with the control perfusate maintained at 37°C and equilibrated with 15% O_2, 6% CO_2, balance N_2 resulting in perfusate pO_2, pCO_2 and pH of ~105 Torr, 40 Torr, and 7.4, respectively. Initially, control perfusate was pumped through the lung until it was evenly blanched and venous effluent was clear of blood. The lung was ventilated (40 breaths/min) with end-inspiratory and end-expiratory pressures of ~ 6 and 3 mmHg,

respectively, with the above gas mixture. The pulmonary arterial pressure was referenced to atmospheric pressure at the level of the left atrium and monitored continuously during the course of the experiments. The venous effluent pressure was atmospheric pressure.

E. Experimental protocols

Lung surface fluorescence measurements—The fluorometer was used in a dark room to minimize stray-light effects [18]. Surface fluorescence was then measured by placing the fiber optic probe against the pleural surface of the right lobe. For a given lung, NADH and FAD surface fluorescence signals were first acquired under resting conditions (lung perfused with control perfusate and ventilated with 6% CO_2 balance O_2 ventilation gas), and then following the addition of one or more of the following agents (rotenone, potassium cyanide, and pentachlorophenol) to the recirculation perfusate. Rotenone (20 μM) was used to inhibit mitochondrial complex I activity (Fig. 2), which would be expected to increase NADH signal by reducing the chain upstream from complex I. As a mitochondrial complex IV inhibitor (Fig. 2), potassium cyanide (KCN, 2 mM) would be expected to reduce the chain upstream from complex IV and hence increase NADH signal, and decrease FAD signal from succinate dehydrogenase (complex II). Uncoupled mitochondrial condition was achieved by the addition of pentachlorophenol (PCP, mitochondrial uncoupler; 3 mM) to the recirculating perfusate. As a protonophore, PCP should oxidize the chain and hence decrease NADH signal and increase FAD signal (Fig. 2). For some of the lungs, KCN was added after the initial addition of rotenone or PCP to the recirculating perfusate. The above concentrations of rotenone, KCN, and PCP were chosen to achieve maximal inhibition or uncoupling and hence maximal changes in NADH and/or FAD signal based upon published reports [11, 18].

At the end of the above imaging protocol, a subset of normoxic and hyperoxic lungs were fixed inflated with paraformaldehye, paraffin embedded, sectioned in 5 micron thick whole mounts, then stained with hematoxylin and eosin (H&E) staining.

F. Fluorescent Signal Processing

The signal measured by the fluorometer contains a time shared sequence of NADH and FAD pulses collected from the surface of the lung. Superimposed over the signal for NADH or FAD is lung ventilation noise. To remove this noise, the trend of the data was first calculated by extracting the maximum value of each pulse. This trend was then smoothed out using a fourth order median filter followed by a fourth order moving average filter. The resulting NADH and FAD signals were then normalized by dividing each by its baseline value (signal level in the absence of any metabolic inhibitor or uncoupler) [18].

G. Complex I and II Assays

For a separate sets of normoxic and hyperoxic lungs the activities of mitochondrial complex I and II were determined as previously described [21, 22]. Briefly, lungs were isolated and washed free of blood with perfusate containing (in mM) 4.7 KCl, 2.51 $CaCl_2$, 1.19 $MgSO_4$, 2.5 KH_2PO_4, 118 NaCl, 25 $NaHCO_3$, 5.5 glucose, and 2.5% Ficoll. Lungs were then removed from the perfusion system, weighed, minced, and homogenized with buffer (pH 7.2) containing (in mM) 225 mannitol, 75 sucrose, 5 3-[N-morpholino] propanesulfonic

acid, 20 ethylene glycol-bis (B-aminoethyl ether)-N,N,N′,N′-tetraacetic acid, 2% fatty-acid free BSA, and 0.02 ml per ml protease inhibitor cocktail set III (Calbiochem, La Jolla, CA), utilizing a Polytron tissue homogenizer. Lung homogenates were centrifuged at 1,500 g for 5 min at 4°C, and the resulting supernatants were centrifuged again at 13,000 g for 30 min at 4°C to obtain a crude mitochondrial fraction (P2). The P2 fractions were washed twice by resuspension in 8 ml ice-cold homogenization buffer without BSA and then centrifuged (13,000 g for 20 min at 4°C). The final P2 fractions were resuspended in 1-ml BSA-free homogenization buffer. Mitochondrial complex I (NADH dehydrogenase) activity (nmol NADH oxidized·min^{-1}·mg protein^{-1}) was determined as the difference between the rates of NADH oxidation in the presence and absence of rotenone over the linear portion of the reaction progress curve as we have previously described [21]. Mitochondrial complex II (succinate-coenzyme Q reductase) activity was determined as the difference between the rates of reduction of the artificial electron acceptor 2,6-dichlorophenolindophenol (DCPIP) in the presence and absence of thenoyltrifluoroacetone (TTFA, complex II inhibitor) over the linear portion with succinate as donor [22]. The protein concentrations were determined colorimetrically as previously described [21].

Statistical evaluation of data—Data are presented as means ± standard error (SE) unless otherwise stated. Statistical comparisons were carried out in each group using paired and unpaired *t*-test as appropriate for design, with $p < 0.05$ as the criterion for statistical significance.

III. Results

Rats did not display any sign of distress after 48 hours of exposure to >95% O_2. Over the course of this exposure period, the rats experienced a small (~3%), but significant loss in body weight (pre- and post-body weights of 337 ± 14 (SE, n = 16) g and 327 ± 13 g, respectively). Histology revealed preserved lung morphology after 48 hours of hyperoxic exposure (Fig. 3).

For both normoxic and hyperoxic lungs, the response of both NADH and FAD lung surface signals to lung perfusion with rotenone, KCN, or PCP appeared within a minute of adding the chemical to the perfusate reservoir (Fig. 4 and Fig. 5). An increase (from baseline) in NADH fluorescence signal indicates reduction of the mitochondrial matrix (Fig. 2), whereas an increase in the FAD fluorescence signal indicates oxidation of the electron transport chain. In this study, the change in NADH signal in the presence of rotenone or KCN is considered a measure of mitochondrial complex I activity, and the change in the FAD signal in the presence of KCN is considered a measure of mitochondrial complex II activity.

For normoxic lungs (Fig. 4 and Table I), lung perfusion with rotenone (complex I inhibitor) reduced the mitochondrial matrix (ETC) upstream from complex I resulting in an increase in NADH signal by 20.2 ± 2.3 (SE) %, with no effect on FAD signal. Lung perfusion with KCN (complex IV inhibitor) reduced the ETC resulting in a 21.7 ± 2.5 % increase in NADH and 6.8 ± 1.6 % decrease in FAD. Lung perfusion with PCP, which uncoupled ETC from phosphorylation, decreased NADH signal by 19.7 ± 2.1% with no effect on FAD signal. The addition of KCN to PCP-treated lungs reversed the effect of PCP on the redox status of the

ETC, increasing NADH signal by 25.7 ± 2.6% and decreasing FAD signal by −9.3 ± 1.0%. In the presence of rotenone, KCN resulted in a small but significant decrease (−3.3 ± 0.8%) in lung surface FAD signal and increase (4.6 ± 1.0%) on NADH signal as compared to values in the presence of rotenone only.

For hyperoxic lungs (Fig. 5, Table I), lung perfusion with rotenone increased NADH signal by 7.5 ± 1.1%, which is 63% lower than in normoxic lungs, with no effect on FAD signal. Lung perfusion with KCN increased NADH by 9.2 ± 1.2%, which is 58% lower than in normoxic lungs. KCN effect on FAD signal in hyperoxic lungs was not significantly different from that in normoxic lungs. Lung perfusion with PCP had the same qualitative and quantitative effects on NADH and FAD signals as in normoxic lungs. The addition of KCN to PCP-treated hyperoxic lungs increased NADH by 9.0 ± 1.0%, which is 65% smaller than that in normoxic lungs. Furthermore, KCN decreased FAD signal by 4.2 ± 0.7%, which is 55% smaller than in normoxic lungs. These results are consistent with a more reduced chain upstream from complex I and II in hyperoxic lungs as compared to normoxic lungs, and suggest a decrease in complex I and II activities in hyperoxic lungs.

Because the data in Table I suggested that the hyperoxic exposure decreased complex I and II activities, we measured the activities of complex I and II in the P2 fractions obtained from lung homogenates. Table II shows that complex I and II activities normalized to protein were ~ 77% and 63% lower, respectively, in P2 fractions derived from hyperoxic than those of normoxic lungs.

IV. Discussion

This study demonstrates the utility of optical fluorescent imaging for evaluating the effect of subacute rat exposure to hyperoxia on the redox state of lung tissue mitochondrial electron transport chain (ETC) in a non-destructive manner in isolated perfused lungs. The results suggest a hyperoxia-induced decrease in complex I and II activities, and demonstrate the ability of this approach to detect a change in mitochondrial redox state in the early phase of hyperoxic lung injury, when histology is not different from that of normoxic rats.

NADH signal and complex I activity

Surface fluorometry results establish that rat exposure to >95% O_2 for 48 hours decreased the change in NADH signal in the presence of KCN or rotenone by 58% and 63%, respectively, as compared to those of normoxic lungs. A similar decrease (65%) in NADH signal was also measured following the addition of KCN to PCP-treated hyperoxic lungs as compared to normoxic lungs. Rotenoneor KCN-induced change in NADH signal is a measure of complex I activity. Thus these result suggest that the ETC upstream from complex I is more reduced in intact hyperoxic lungs than in normoxic lungs, and that complex I activity is lower in hyperoxic lungs. This is consistent with the 77% decrease in mitochondrial complex I activity per mg protein which we measured in P2 fractions derived from hyperoxic lungs as compared to normoxic lung.

The measured hyperoxia-induced change in complex I redox state (Table 2) could be due to a change in complex I protein and/or a change in the rate of NADH production. The latter

could result from impairment to the Krebs cycle and/or change in cytoslic NADH/NAD^+ which could affect mitochondrial NADH level via the malate-aspartate shuttle. However, the hyperoxia-induced change in complex I redox state is most likely due to a change in complex I protein since for the complex I assay (P2 fraction), the NADH concentration used was the same for both normoxic and hyperoxic lung mitochondrial preparations (P2 fractions). The results of this assay (Table 2) show that the measured hyperoxia-induced change in complex I activity is qualitatively and quantitatively consistent with the hyperoxia-induced change in complex I redox state measured on the surface of the lung (Table 1).

The sulfhydryl-containing Krebs cycle enzymes pyruvate and alpha-ketoglutarate dehydrogenase and their coenzymes Coenzyme-A (CoA) and lipoic acid are sensitive to oxidative stress [23]. Previous studies evaluated the effect of rat exposure to 100% O_2 for 24 hrs on these and other Krebs cycle enzymes [15, 23, 24]. Gardner et al. [24] reported a 73% decrease in lung aconitase activity after 24 hrs of rate exposure to 100% O_2. This decrease is consistent with the increase in citrate level (aconitase substrate) in lung tissue under the same exposure conditions as reported by Bassett et al. [23]. This impairment to the Krebs cycle could affect NADH supplied to the electron transport chain and in turn complex I redox state. However it is not known whether this impairment to aconitase activity persists after 48 hrs of exposure to 100% O_2 or whether it is sufficient to account for the measured hyperoxia-induced change in complex I redox state. In another study, Bassett et al. [15] reported that rat exposure to 100% O_2 for 24 hrs had no effect on the activities of the Krebs cycle enzymes succinate dehydrogenase, isocitrate dehydrogenase or α-glycerophosphate dehydrogenase. In the present study we report a 64% decrease in succinate dehydrogenase (complex II) activity after 48 hrs of exposure to 100% O_2. Additional studies would be needed to evaluate the effect of rat exposure to 100% O_2 for 48 hrs on the activities of Krebs cycle enzymes isocitrate dehydrogenase, α-glycerophosphate dehydrogenase, and aconitase to determine the potential contribution of impaired production of NADH by the Krebs cycle to the measured change in complex I redox state.

Fisher AB [16] reported that rat exposure to 100% O_2 for 48 hrs increased lung lactate production rate (78%) and lactate to pyruvate ratio (108%). Since lactate to pyruvate ratio is proportional to cytosolic NADH/NAD^+, the increase in lactate to pyruvate ratio suggests an increase in cytosolic NADH transported to the mitochondria matrix via the malate-aspartate shuttle. This shuttle provide more cytosolic NADH to mitochondria when the cytosolic NADH/NAD^+ is higher than in the mitochondrial matrix. Thus the hyperoxia-induced increase in cytosolic NADH/NAD^+ could contribute to the measured change in complex I redox state in hyperoxic lungs.

Rat exposure to hyperoxia had no effect on the change in NADH signal in the presence of PCP as compared to that in normoxic lungs as a measure of the coupling between ETC and phosphorylation. This observation implies that rat treatment with hyperoxia (>95% O_2 for 48 hours) did not alter the coupling between respiration and phosphorylation in lung tissue despite the apparent decrease in complex I activity. However, since the ETC upstream from complex I is more reduced in hyperoxic lungs than in normoxic lungs, one would expect a larger PCP-induced decrease in NADH signal in hyperoxic lung. Currie et al. demonstrated

that rat exposure to 100% O_2 for 48 hours decreased ADP-stimulated O_2 consumption (state 3) by ~50% with aketoglutarate as an NAD-linked substrate [25]. Together these results support a decreased tightness of coupling between respiration and phosphorylation in hyperoxic lungs as compared to normoxic lungs.

There is ample evidence that increased production of reactive oxygen species (ROS) is a major pathophysiological factor in the genesis of hyperoxic lung injury [3, 26–28]. Thus, one strategy that cells may have evolved to protect against hyperoxic lung injury is to mitigate the activities of ROS sources [12, 29–31]. Mitochondrial electron transport complex I is a major source of ROS [3, 27, 32]. Moreover, studies have shown that the rate of ROS formation at complex I in endothelial cells increased with an increase in O_2 tension, and that complex I inactivation using rotenone decreased ROS generation in sheep pulmonary microvascular endothelial cells exposed to hyperoxia (100% O_2 for 30 min) [27, 32, 33]. Thus the measured decrease in complex I could be an adaptive mechanism by the cells to decrease the rate of ROS formation at complex I under hyperoxic conditions.

On the other hand, the measured decrease in complex I activity could represent hyperoxia-induced injury leading to increases in the rate of ROS formation. Mitochondrial DNA (mDNA) is highly sensitive to ROS [34]. Hyperoxia-induced increase in the rate of ROS formation could damage mDNA and as a result compromise complex I activity since 7 out of 45 subunits of complex I are encoded by mDNA [34, 35]. Hyperoxia-induced increase in ROS formation could also cause direct damage to complex I activity by oxidizing cardiolipin, which is sensitive to ROS [36, 37]. This phospholipid is important for the function of complex I [38]. In addition, oxidation of this lipid could lead to increase in the loss of electrons at complex I and in the rate of mitochondrial superoxide formation at complex I [36, 37].

Ratner et al. demonstrated that exposure of neonatal mice to hyperoxia (75% O_2 for 72 hours) decreases complex I activity by ~70%, and that this decrease compromises mitochondrial oxidative phosphorylation and contributes to alveolar development arrest [7]. Fisher AB [16] showed that rat exposure to 100% O_2 for 48 hours had no effect on lung tissue ATP content as compared to normoxic lungs, although there was an increase (105%) in lactate/pyruvate ratio indicating an increase in ATP production via glycolysis. He suggested that the increased lactate/pyruvate ratio could be due to demand for glycolytic ATP and/or decrease in ATP production via oxidative phosphorylation which is compensated for by an increase in ATP production via glycolysis.

FAD signal and complex II activity

Compared to NADH, the measured change in the FAD signal in response to lung treatment with the metabolic inhibitors was relatively small for normoxic and hyperoxic lungs (Table 1). One reason for this observation could be lower lung tissue concentration of FAD as compared to NADH. In fact, the FAD baseline signal is small relative to the NADH signal as evidenced by the difference in signal amplification for the NADH and FAD channels (10^3 for NADH compared to ~6×10^5 for FAD) [18].

Lung treatment with KCN, which reduces the ETC upstream from complex IV, should reduce complex II and as a result decrease FAD signal. Just as a change in NADH tracks complex I activity, a change in FAD signal reflect complex II activity. Rat exposure to hyperoxia had no significant effect on the change in FAD signal in the presence of KCN as compared to that in lungs from normoxic rats. However, the change in FAD signal following the addition of KCN to PCP-treated lungs was 56% lower in hyperoxic lungs than normoxic lungs. It could be that lung treatment with PCP, which simulates the flow of reducing equivalents through the chain, fully oxidized the chain and as a result exposed the difference in the capacities of complex II between normoxic and hyperoxic lungs. Regardless, this apparent decrease in complex II activity is consistent with the 63% decrease in mitochondrial complex II activity per mg protein in P2 fractions derived from hyperoxic lungs as compared to normoxic lung (Table 2).

The measured hyperoxia-induced change in FAD signal in the presence of (PCP + KCN) could be due to a direct oxidant-induced inhibition of complex II or indirect inhibition of complex II by impairment of Krebs cycle enzymes/coenzymes that result in a decrease in succinate concentration or increase in the concentration of oxaloacetate (OAA). Complex II activity is inhibited by a high level of OAA. However the results of the mitochondrial isolates (P2 fractions) suggest that the hyperoxia-induced change in complex II redox state is most likely due to impairment of complex II itself since for this assay the concentrations of succinate and the electron acceptor (DCPIP) used were the same for the mitochondrial isolates from both normoxic and hyperoxic lungs and should be in excess of what is required for maximal function of complex II. The measured decrease in complex II activity using this assay (Table 2) is qualitatively and quantitatively consistent with the measured hyperoxia-induced decrease in FAD signal in the presence of PCP + KCN as a measure of complex II activity (Table 1).

Complex II is the only ETC complex that is completely encoded by nuclear DNA [39]. Hence, damage to mDNA due to hyperoxia-induced increase in the rate of ROS formation should have no effect on complex II. Since electrons channeled through complex II produce 4-fold more mitochondrial superoxide than electrons channeled through complex I [40], the apparent decrease in complex II activity could be a means by the cells to reduce ROS formation under hyperoxic conditions.

Additional studies are needed to evaluate the effect of the depression in complex I and complex II activities observed in hyperoxic lungs on ROS production at complex I and III and mitochondrial bioenergetics, and to determine whether this depression is an injury or an adaptive response to the hyperoxic environment.

Sources of NADH and FAD surface fluorescent signals

Our assumption in this study is that changes in the mitochondrial pool of NADH is a key contributor to the measured changes in the NADH fluorescence signal since the metabolic inhibitors we used target the mitochondrial electron transport chain [18]. Another source of NADH signal is the cytosolic pool of NADH. Fisher et al. [41] demonstrated that rat lung treatment with KCN increased lung lactate/pyruvate by 4-fold. In this study, lung perfusion with KCN increased lung surface NADH signal by 22% in normoxic lungs. Since lactate/

pyruvate ratio reflects cytosolic NADH/NAD^+ [42, 43], this suggests that cytosolic NADH did not contribute significantly to the measured lung surface NADH signal.

Unlike the NADH signal which has cytosolic and mitochondrial components, the FAD signal derives only from the mitochondria [18, 44]. Sources of redox-sensitive flavoprotein (FAD) include succinate dehydrogenase (complex II), lipoamide dehydrogenase (LipDH), and electron transfer flavoprotein (ETF) [18, 45, 46]. However, as previously discussed, most of the measured lung surface FAD signal is from complex II flavin [18].

Fisher AB demonstrated that rat exposure to 100% O_2 for 48 hours stimulated glycolysis as measured by ~105% increase in the lung lactate/pyruvate ratio [16]. Since this ratio is a measure of cytosolic NADH/NAD^+, this suggest that lung tissue cytoplasm is more reduced in hyperoxic lungs than normoxic lungs. Thus, coupled with the results of the present study, the data document that both tissue cytosolic and mitochondrial matrix are more reduced in hyperoxic lungs than normoxic lungs.

The hyperoxia-induced decrease in complex I and II activities in the present study represents a relatively early *in situ* metabolic consequence of hyperoxia in that it precedes effects on lung histology, hemodynamic and functional endpoints observed with rat exposure to >95% O_2 for > 48 hours [8, 47]. Of the few studies evaluating the metabolic consequences of hyperoxia in the 18–48 hr period, a decrease in serotonin clearance and an increase in lactate production have been observed in lungs from rats exposed to 100% O_2 for 18 and 36 hrs, respectively/[16, 48]. Audi et al. reported that rat exposure to hyperoxia (85% O_2 for 48 hours) results in 47% decrease in the capacity of complex I mediated coenzyme Q_1 (amphipathic homolog of ubiquinone) reduction on passages through the pulmonary circulation as compared to that in lungs of normoxic rats [11]. Additionally, Klein et al. demonstrated a decrease in the metabolism of prostaglandin E_2 metabolism in intact lungs of rats exposed to > 97% O_2 for 36 hrs [49].

Limitations and potential solutions

In the present study and previous studies by us and other [18, 50–52], the relative change in the NADH and FAD signals are reported instead of the actual signals which are sensitive to various factors including probe distance from the organ surface, day-to-day variations in light intensity, and PMT gain settings. One approach to overcoming this limitation would be by imaging a phantom of known NADH and FAD concentrations at the end of a given experiment (lung), and then use this information to scale the measured NADH and FAD signals. This would allow us to compare un-normalized signals from different lungs.

The lung surface optical imaging data does not provide information about the specific types of lung cells contributing to the measured NADH and FAD signals, although endothelial cells would be expected to contribute significantly because of their relatively large surface area and fraction of total lung cells [8]. Although determining the contributions of specific lung cell types to the measured signal is potentially important, the global oxidoreductive state of the lung tissue is a highly valuable piece of information irrespective of the individual cell types contributing to the redox ratio.

Another limitation of lung surface optical imaging is that it *may* not detect deeper than 500 μm, with a diameter of 3.2 mm, for a volume of ~ 4 mm^3. However, this resolution is more than sufficient for determining the RR of parenchymal tissue which has a thickness (air to plasma) of 1.6 μm [8]. That said, central lung lesions without pleural extension would not be expected to be detected by surface fluorescence measurements such as those used in the present study.

V. Clinical and Translational significance

Over 900,000 adults receive invasive mechanical ventilation (MV) in the United States each year [53, 54]. Many either have acute lung injury (ALI) or have conditions such as shock and severe sepsis that place them at particular risk of ALI [54–59]. Treatment with high fractions of oxygen to maintain adequate tissue oxygenation may further exacerbate lung injury. However susceptibilities to lung injury (from hyperoxia or shock) are widely variable from person to person, and there are only crude means of screening for or following these injuries clinically.

The results of this study suggest that hyperoxia-induced mitochondrial dysfunction occurs prior to the inflammatory phase of lung O_2 toxicity. If so, a change in lung surface mitochondrial redox state measured using optical fluorescence techniques could be used as an index of lung O_2 toxicity in patients with ALI requiring high oxygen therapy or to monitor the progression of ALI and its most severe form Acute Respiratory Distress Syndrome (ARDS), one of the most frequent causes of admission to the intensive care unit [60]. The fiber optic probe could be placed on the lung pleural surface through a small thoracotomy incision or a thoracostomy tube in patients with these devices in place. Alternatively, the probe might be introduced through an endotracheal tube, and positioned against airway epithelium. The same probe could be used to evaluate the efficacy of novel or existing interventions on lung tissue mitochondrial redox state and energy homeostasis in real time.

An individual with enhanced susceptibility to ARDS would be a strong candidate for strategies such as scrupulous attention to ventilation with low tidal volumes, deliberate tolerance of lower arterial oxygen or higher carbon dioxide tensions to limit oxygen toxicity or barotrauma, avoidance of transfusions, etc [53–59]. These interventions decrease injury but incur additional risks (increased sedation, impairment of vital organ function) that limit their universal and strict application in ALI patients.

The diagnostic and therapeutic monitoring applications of this tool are important not only for ALI/ARDS, but also for other lung conditions including lung cancer which is characterized by mitochondrial impairment (so called Warburg effect) [61], lung transplant related ischemia-reperfusion injury [62], or other animal models of human ALI [63]. Additional applications include diagnostic and therapeutic monitoring of conditions in other organs with high energy flux such as heart ischemia-reperfusion injury and heart failure management [64–66], or intraoperative identification of ischemic intestine and others [67].

Acknowledgments

This work was supported in part by the support of University of Wisconsin Milwaukee RGI 7 Grant, Clinical and Translational Science Institute KL2 Grant: NIH 8Kl2TR000056, Wisconsin Applied Research grant (Wi-ARG), NIH grant 8UL1TR000055 (CTSI), VA Merit Review Award BX001681, and the Department of Veterans Affairs that provided resources essential to the completion of these investigations.

We appreciate the technical help from Robert Bongard, and input from Dr. Marilyn Merker in the Clement J. Zablocki VA, Milwaukee, WI.

References

1. Saugstad OD. Optimal oxygenation at birth and in the neonatal period. Neonatology. 2007; 91:319–22. [PubMed: 17575477]
2. Dunne PJ, Macintyre NR, Schmidt UH, Haas CF, Jones-Boggs Rye K, Kauffman GW, Hess DR. Respiratory care year in review 2011: long-term oxygen therapy, pulmonary rehabilitation, airway management, acute lung injury, education, and management. Respir Care. 57:590–606. [PubMed: 22472499]
3. Kallet RH, Matthay MA. Hyperoxic acute lung injury. Respir Care. 2013; 58:123–41. [PubMed: 23271823]
4. Davis WB, Rennard SI, Bitterman PB, Crystal RG. Pulmonary oxygen toxicity. Early reversible changes in human alveolar structures induced by hyperoxia. N Engl J Med. 1983; 309:878–83. [PubMed: 6888481]
5. Fisher AB, Beers MF. Hyperoxia and acute lung injury. Am J Physiol Lung Cell Mol Physiol. 2008; 295:L1066. author reply L1067. [PubMed: 19047485]
6. O'Brodovich HM, Mellins RB. Bronchopulmonary dysplasia. Unresolved neonatal acute lung injury. Am Rev Respir Dis. 1985; 132:694–709. [PubMed: 3898946]
7. Ratner V, Starkov A, Matsiukevich D, Polin RA, Ten VS. Mitochondrial dysfunction contributes to alveolar developmental arrest in hyperoxia-exposed mice. Am J Respir Cell Mol Biol. 2009; 40:511–8. [PubMed: 19168698]
8. Crapo JD, Barry BE, Foscue HA, Shelburne J. Structural and biochemical changes in rat lungs occurring during exposures to lethal and adaptive doses of oxygen. Am Rev Respir Dis. 1980; 122:123–43. [PubMed: 7406333]
9. Crapo JD, Peters-Golden M, Marsh-Salin J, Shelburne JS. Pathologic changes in the lungs of oxygen-adapted rats: a morphometric analysis. Lab Invest. 1978; 39:640–53. [PubMed: 739764]
10. Zmijewski JW, Lorne E, Zhao X, Tsuruta Y, Sha Y, Liu G, Siegal GP, Abraham E. Mitochondrial respiratory complex I regulates neutrophil activation and severity of lung injury. Am J Respir Crit Care Med. 2008; 178:168–79. [PubMed: 18436790]
11. Audi SH, Merker MP, Krenz GS, Ahuja T, Roerig DL, Bongard RD. Coenzyme Q1 redox metabolism during passage through the rat pulmonary circulation and the effect of hyperoxia. J Appl Physiol. 2008; 105:1114–26. [PubMed: 18703762]
12. Gan Z, Roerig DL, Clough AV, Audi SH. Differential responses of targeted lung redox enzymes to rat exposure to 60 or 85% oxygen. J Appl Physiol. 2011; 111:95–107. [PubMed: 21551015]
13. Gan Z, Audi SH, Bongard RD, Gauthier KM, Merker MP. Quantifying mitochondrial and plasma membrane potentials in intact pulmonary arterial endothelial cells based on extracellular disposition of rhodamine dyes. Am J Physiol Lung Cell Mol Physiol. 2011; 300:L762–72. [PubMed: 21239539]
14. Bassett DJ, Bowen-Kelly E, Reichenbaugh SS. Rat lung glucose metabolism after 24 h of exposure to 100% oxygen. J Appl Physiol. 1989; 66:989–96. [PubMed: 2496080]
15. Bassett DJ, Elbon CL, Reichenbaugh SS. Respiratory activity of lung mitochondria isolated from oxygen-exposed rats. Am J Physiol. 1992; 263:L439–45. [PubMed: 1415721]
16. Fisher AB. Energy status of the rat lung after exposure to elevated PO2. J Appl Physiol. 1978; 45:56–9. [PubMed: 670032]

17. Audi SH, Bongard RD, Krenz GS, Rickaby DA, Haworth ST, Eisenhauer J, Roerig DL, Merker MP. Effect of chronic hyperoxic exposure on duroquinone reduction in adult rat lungs. Am J Physiol Lung Cell Mol Physiol. 2005; 289:L788–97. [PubMed: 15994278]
18. Staniszewski K, Audi SH, Sepehr R, Jacobs ER, Ranji M. Surface fluorescence studies of tissue mitochondrial redox state in isolated perfused rat lungs. Ann Biomed Eng. 2013; 41:827–36. [PubMed: 23238793]
19. Fisher AB. Intermediary metabolism of the lung. Environ Health Perspect. 1984; 55:149–58. [PubMed: 6376097]
20. Ramanujam N, Richards-Kortum R, Thomsen S, Mahadevan-Jansen A, Follen M, Chance B. Low Temperature Fluorescence Imaging of Freeze-trapped Human Cervical Tissues. Opt Express. 2001; 8:335–43. [PubMed: 19417824]
21. Audi SH, Roerig DL, Haworth ST, Clough AV. Role of Glutathione in Lung Retention of 99mTc-Hexamethylpropyleneamine Oxime in Two Unique Rat Models of Hyperoxic Lung Injury. J Appl Physiol. 2012; 113:658–65. [PubMed: 22628374]
22. Barrientos A, Fontanesi F, Diaz F. Evaluation of the mitochondrial respiratory chain and oxidative phosphorylation system using polarography and spectrophotometric enzyme assays. Curr Protoc Hum Genet. 2009; Chapter 19(Unit19 3)
23. Bassett DJ, Reichenbaugh SS. Tricarboxylic acid cycle activity in perfused rat lungs after O2 exposure. Am J Physiol. 1992; 262:L495–501. [PubMed: 1314504]
24. Gardner PR, Nguyen DD, White CW. Aconitase is a sensitive and critical target of oxygen poisoning in cultured mammalian cells and in rat lungs. Proc Natl Acad Sci U S A. 1994; 91:12248–52. [PubMed: 7991614]
25. Currie WD, Pratt PC, Sanders AP. Hyperoxia and lung metabolism. Chest. 1974; 66(suppl):19S–21S. [PubMed: 4366290]
26. Bhandari V. Molecular mechanisms of hyperoxia-induced acute lung injury. Front Biosci. 2008; 13:6653–61. [PubMed: 18508685]
27. Brueckl C, Kaestle S, Kerem A, Habazettl H, Krombach F, Kuppe H, Kuebler WM. Hyperoxia-induced Reactive Oxygen Species Formation in Pulmonary Capillary Endothelial Cells in situ. Am J Respir Cell Mol Biol. 2005
28. Fisher AB, Forman HJ, Glass M. Mechanisms of pulmonary oxygen toxicity. Lung. 1984; 162:255–9. [PubMed: 6392761]
29. Zhao HW, Ali SS, Haddad GG. Does hyperoxia selection cause adaptive alterations of mitochondrial electron transport chain activity leading to a reduction of superoxide production? Antioxid Redox Signal. 2012; 16:1071–6. [PubMed: 22229946]
30. Campian JL, Qian M, Gao X, Eaton JW. Oxygen tolerance and coupling of mitochondrial electron transport. J Biol Chem. 2004; 279:46580–7. [PubMed: 15328348]
31. Li J, Gao X, Qian M, Eaton JW. Mitochondrial metabolism underlies hyperoxic cell damage. Free Radic Biol Med. 2004; 36:1460–70. [PubMed: 15135183]
32. Turrens JF. Mitochondrial formation of reactive oxygen species. J Physiol. 2003; 552:335–44. [PubMed: 14561818]
33. Sanders SP, Zweier JL, Kuppusamy P, Harrison SJ, Bassett DJ, Gabrielson EW, Sylvester JT. Hyperoxic sheep pulmonary microvascular endothelial cells generate free radicals via mitochondrial electron transport. J Clin Invest. 1993; 91:46–52. [PubMed: 8380815]
34. Ruchko M, Gorodnya O, LeDoux SP, Alexeyev MF, Al-Mehdi AB, Gillespie MN. Mitochondrial DNA damage triggers mitochondrial dysfunction and apoptosis in oxidant-challenged lung endothelial cells. Am J Physiol Lung Cell Mol Physiol. 2005; 288:L530–5. [PubMed: 15563690]
35. Swalwell H, Kirby DM, Blakely EL, Mitchell A, Salemi R, Sugiana C, Compton AG, Tucker EJ, Ke BX, Lamont PJ, Turnbull DM, McFarland R, Taylor RW, Thorburn DR. Respiratory chain complex I deficiency caused by mitochondrial DNA mutations. Eur J Hum Genet. 2011; 19:769–75. [PubMed: 21364701]
36. Paradies G, Petrosillo G, Pistolese M, Ruggiero FM. Reactive oxygen species affect mitochondrial electron transport complex I activity through oxidative cardiolipin damage. Gene. 2002; 286:135–41. [PubMed: 11943469]

37. Chicco AJ, Sparagna GC. Role of cardiolipin alterations in mitochondrial dysfunction and disease. Am J Physiol Cell Physiol. 2007; 292:C33–44. [PubMed: 16899548]
38. Huang L, Tang D, Yappert MC, Borchman D. Oxidation-induced changes in human lens epithelial cells 2. Mitochondria and the generation of reactive oxygen species. Free Radic Biol Med. 2006; 41:926–36. [PubMed: 16934675]
39. Ide T, Tsutsui H, Hayashidani S, Kang D, Suematsu N, Nakamura K, Utsumi H, Hamasaki N, Takeshita A. Mitochondrial DNA damage and dysfunction associated with oxidative stress in failing hearts after myocardial infarction. Circ Res. 2001; 88:529–35. [PubMed: 11249877]
40. Barrientos A, Moraes CT. Titrating the effects of mitochondrial complex I impairment in the cell physiology. J Biol Chem. 1999; 274:16188–97. [PubMed: 10347173]
41. Fisher AB, Furia L, Chance B. Evaluation of redox state of isolated perfused rat lung. Am J Physiol. 1976; 230:1198–1204. [PubMed: 5896]
42. Suranadi IW, Demaison L, Chate V, Peltier S, Richardson M, Leverve X. An increase in the redox state during reperfusion contributes to the cardioprotective effect of GIK solution. J Appl Physiol. 2012; 113:775–84. [PubMed: 22797310]
43. Nuutinen EM. Subcellular origin of the surface fluorescence of reduced nicotinamide nucleotides in the isolated perfused rat heart. Basic Res Cardiol. 1984; 79:49–58. [PubMed: 6233965]
44. Aldakkak M, Stowe DF, Lesnefsky EJ, Heisner JS, Chen Q, Camara AK. Modulation of mitochondrial bioenergetics in the isolated Guinea pig beating heart by potassium and lidocaine cardioplegia: implications for cardioprotection. J Cardiovasc Pharmacol. 2009; 54:298–309. [PubMed: 19620879]
45. Kunz WS, Kunz W. Contribution of different enzymes to flavoprotein fluorescence of isolated rat liver mitochondria. Biochim Biophys Acta. 1985; 841:237–46. [PubMed: 4027266]
46. Kunz WS, Gellerich FN. Quantification of the content of fluorescent flavoproteins in mitochondria from liver, kidney cortex, skeletal muscle, and brain. Biochem Med Metab Biol. 1993; 50:103–10. [PubMed: 8373630]
47. Frank L, Iqbal J, Hass M, Massaro D. New “rest period” protocol for inducing tolerance to high O2 exposure in adult rats. Am J Physiol. 1989; 257:L226–31. [PubMed: 2801950]
48. Block ER, Fisher AB. Depression of serotonin clearance by rat lungs during oxygen exposure. J Appl Physiol. 1977; 42:33–8. [PubMed: 833074]
49. Klein LS, Fisher AB, Soltoff S, Coburn RF. Effect of O2 exposure on pulmonary metabolism of prostaglandin E2. Am Rev Respir Dis. 1978; 118:622–5. [PubMed: 707883]
50. Chance B, Legallais V, Sorge J, Graham N. A versatile time-sharing multichannel spectrophotometer, reflectometer, and fluorometer. Anal Biochem. 1975; 66:498–514. [PubMed: 166573]
51. Matsubara M, Ranji M, Leshnower BG, Noma M, Ratcliffe SJ, Chance B, Gorman RC, Gorman JH 3rd. In vivo fluorometric assessment of cyclosporine on mitochondrial function during myocardial ischemia and reperfusion. Ann Thorac Surg. 2010; 89:1532–7. [PubMed: 20417773]
52. Mayevsky A, Rogatsky GG. Mitochondrial function in vivo evaluated by NADH fluorescence: from animal models to human studies. Am J Physiol Cell Physiol. 2007; 292:C615–40. [PubMed: 16943239]
53. Wunsch H, Linde-Zwirble WT, Angus DC, Hartman ME, Milbrandt EB, Kahn JM. The epidemiology of mechanical ventilation use in the United States. Crit Care Med. 2010; 38:1947–53. [PubMed: 20639743]
54. Kumar G, Majumdar T, Jacobs ER, Danesh V, Dagar G, Deshmukh A, Taneja A, Nanchal R. Outcomes of morbidly obese patients receiving invasive mechanical ventilation: a nationwide analysis. Chest. 2013; 144:48–54. [PubMed: 23349057]
55. Gajic O, Dara SI, Mendez JL, Adesanya AO, Festic E, Caples SM, Rana R, St Sauver JL, Lymp JF, Afessa B, Hubmayr RD. Ventilator-associated lung injury in patients without acute lung injury at the onset of mechanical ventilation. Crit Care Med. 2004; 32:1817–24. [PubMed: 15343007]
56. Trillo-Alvarez C, Cartin-Ceba R, Kor DJ, Kojicic M, Kashyap R, Thakur S, Thakur L, Herasevich V, Malinchoc M, Gajic O. Acute lung injury prediction score: derivation and validation in a population-based sample. Eur Respir J. 2011; 37:604–9. [PubMed: 20562130]

57. Rubenfeld GD, Caldwell E, Peabody E, Weaver J, Martin DP, Neff M, Stern EJ, Hudson LD. Incidence and outcomes of acute lung injury. N Engl J Med. 2005; 353:1685–93. [PubMed: 16236739]

58. Nagase T, Uozumi N, Ishii S, Kume K, Izumi T, Ouchi Y, Shimizu T. Acute lung injury by sepsis and acid aspiration: a key role for cytosolic phospholipase A2. Nat Immunol. 2000; 1:42–6. [PubMed: 10881173]

59. Elie-Turenne MC, Hou PC, Mitani A, Barry JM, Kao EY, Cohen JE, Frendl G, Gajic O, Gentile NT. Lung injury prediction score for the emergency department: first step towards prevention in patients at risk. Int J Emerg Med. 2012; 5:33. [PubMed: 22943391]

60. Phua J, Badia JR, Adhikari NK, Friedrich JO, Fowler RA, Singh JM, Scales DC, Stather DR, Li A, Jones A, Gattas DJ, Hallett D, Tomlinson G, Stewart TE, Ferguson ND. Has mortality from acute respiratory distress syndrome decreased over time?: A systematic review. Am J Respir Crit Care Med. 2009; 179:220–7. [PubMed: 19011152]

61. Panngom K, Baik KY, Nam MK, Han JH, Rhim H, Choi EH. Preferential killing of human lung cancer cell lines with mitochondrial dysfunction by nonthermal dielectric barrier discharge plasma. Cell Death Dis. 4:e642. [PubMed: 23703387]

62. Sommer SP, Sommer S, Sinha B, Wiedemann J, Otto C, Aleksic I, Schimmer C, Leyh RG. Ischemia-reperfusion injury-induced pulmonary mitochondrial damage. J Heart Lung Transplant. 2011; 30:811–8. [PubMed: 21470877]

63. Matute-Bello G, Frevert CW, Martin TR. Animal models of acute lung injury. Am J Physiol Lung Cell Mol Physiol. 2008; 295:L379–99. [PubMed: 18621912]

64. Kevin LG, Novalija E, Riess ML, Camara AK, Rhodes SS, Stowe DF. Sevoflurane exposure generates superoxide but leads to decreased superoxide during ischemia and reperfusion in isolated hearts. Anesth Analg. 2003; 96:949–55. table of contents. [PubMed: 12651639]

65. Ranji M, Matsubara M, Leshnower BG, Hinmon RH, Jaggard DL, Chance B, Gorman RC, Gorman JH III . Quantifying acute myocardial injury using ratiometric fluorometry. IEEE Trans Biomed Eng. 2009; 56:1556–63. [PubMed: 19272908]

66. Ince C, Coremans JM, Bruining HA. In vivo NADH fluorescence. Adv Exp Med Biol. 1992; 317:277–96. [PubMed: 1288134]

67. Ince C, van der Sluijs JP, Sinaasappel M, Avontuur JA, Coremans JM, Bruining HA. Intestinal ischemia during hypoxia and experimental sepsis as observed by NADH videofluorimetry and quenching of Pd-porphine phosphorescence. Adv Exp Med Biol. 1994; 361:105–10. [PubMed: 7597932]

Biographies

Reyhaneh Sepehr obtained her B.S. and her M.S. in biomedical engineering from Amirkabir university of technology (Tehran, Iran) and currently is a PhD candidate in electrical engineering department at the university of Wisconsin Milwaukee. The focus of her research in Biophotonics Laboratory is on optical studies of the metabolic status of different tissues and mostly on signal and image processing techniques and algorithms.

Said Audi is an Associate Professor of Biomedical Engineering at Marquette University. Dr. Audi's research interest has been primary in mathematical modeling of physiologic systems, including in the areas of pulmonary mass transfer, pulmonary hemodynamics, and functional imaging. Dr. Audi's research focuses on using indicator dilution techniques, optical fluorescence and single photon emission computed tomography (SPECT) imaging, as well as computational modeling to elucidate the underlying mechanisms of acute lung injury.

Kevin S. Staniszewski obtained his B.S. in Electrical Engineering from the University of Wisconsin Milwaukee, in December of 2009. He then continued to obtain his M.S. in Electrical Engineering from the same university with a concentration in biophotonics.

He began working in the industry with a Test Engineer Internship at Cooper Power Systems in Summer 2009. After finishing his graduate studies, he continued to work as a Research Associate in the Biophotonics Laboratory at the University of Wisconsin Milwaukee. He is currently employed as a Software Engineer at Prairie Technologies, Inc in Middleton, Wisconsin.

Steven T. Haworth is Research Scientist in Pulmonary and Critical Care Medicine at the Medical College of Wisconsin and Research Engineer at the Zablocki VA Medical Center. His interests focus on using a range of medical imaging modes (microcomputed tomography, micro single-photon emission computed tomography) as tools for

understanding the overall structural, functional and metabolic relationships of the pulmonary vascular system under various compromised diseased states.

Elizabeth R. Jacobs is a Professor of Pulmonary and Critical Care Medicine at the Medical College of Wisconsin and the Associate Chief of Staff at the Zablocki VA Medical Center. Her interest is in mechanisms underlying acute lung injury as well as novel diagnostics to better identify pulmonary injury.

Mahsa Ranji is an Assistant Professor in Electrical Engineering department at University of Wisconsin-Milwaukee. She is the director of Biophotonics Laboratory with research focus on optical imaging, and image processing of tissue metabolism. Her group has implemented optical devices to study cardiopulmonary injuries. She is a member of IEEE.

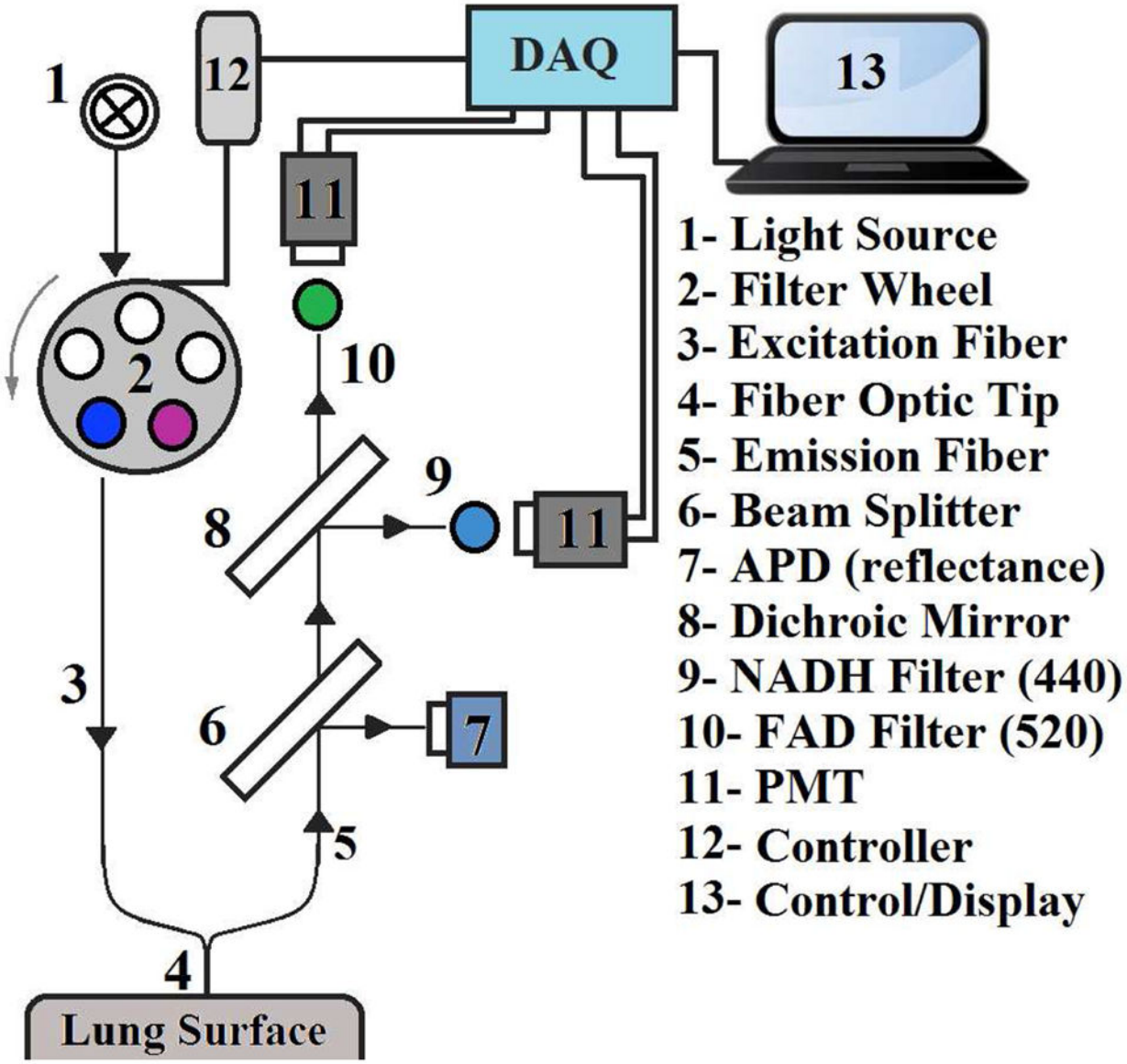

Fig. 1.
Schematic of the Fluorometer.

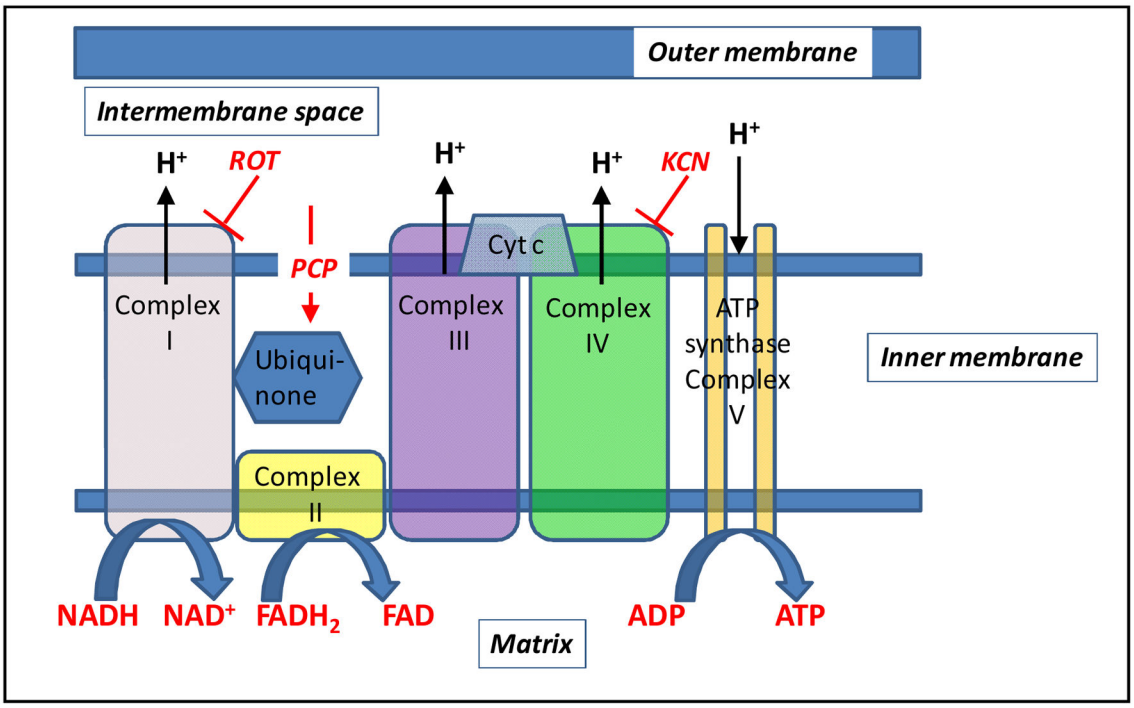

Fig. 2.

Schematic representation of subunits of mitochondrial oxidative phosphorylation complexes. Hydrogen ions are transported from the mitochondrial matrix across the inner mitochondrial membrane into the intermembrane space by complexes I, III, and IV. The movement of hydrogen ions down the electrochemical gradient is coupled to the phosphorylation of adenosine diphosphate (ADP) to form adenosine triphosphate (ATP) by complex V. Electrons from the autofluorescent reducing agent, nicotine adenine dinucleotide (NADH), move from complex I through ubiquinone to complex III and then complex IV via cytochrome c (Cyt c). Electrons from succinate, another reducing agent, enter the respiratory chain through flavin adenine dinucleotide (FAD), which is covalently linked to complex II of the respiratory chain. Like NADH, the reduced form of FAD (FADH) is autofluorescent. Rotenone (ROT) and potassium cyanide (KCN) inhibit complex I and IV, respectively. Pentachlorophenol (PCP) is a protonophore which increases membrane proton conductivity, disrupts the proton gradient across the membrane, and as a result uncouples mitochondrial electron transport chain from phosphorylation.

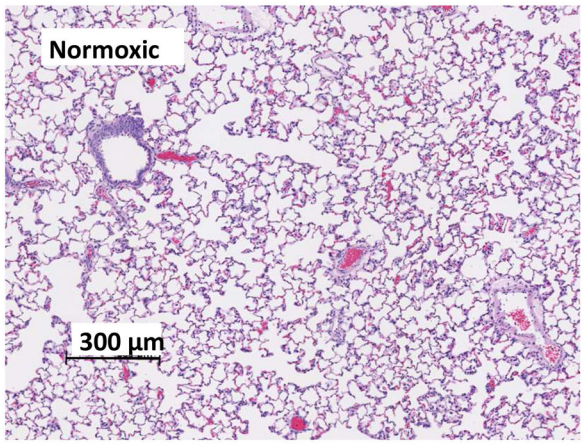

(a)

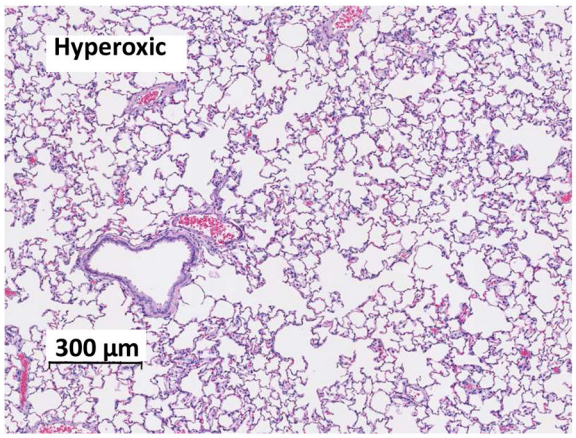

(b)

Fig. 3.

Histology: Images of H&E section of normoxic (a) vs. hyperoxic (b) lungs. After 48 hours of exposure, lungs show no evidence of neutrophilic infiltrates, pulmonary edema, or vascular smooth muscle thickening, which are characteristic of hyperoxic injury sustained after rat exposure for 60 hours or longer.

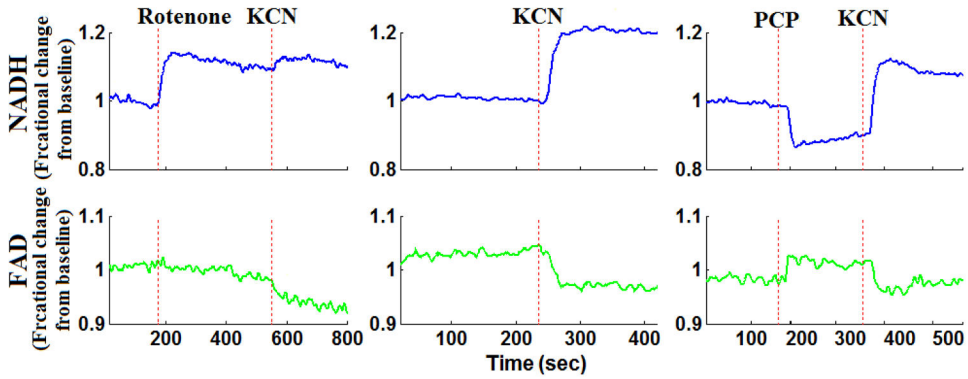

Fig. 4.

Representative fluorometer response to perfusion with chemical inhibitors and uncouplers in a normoxic lung

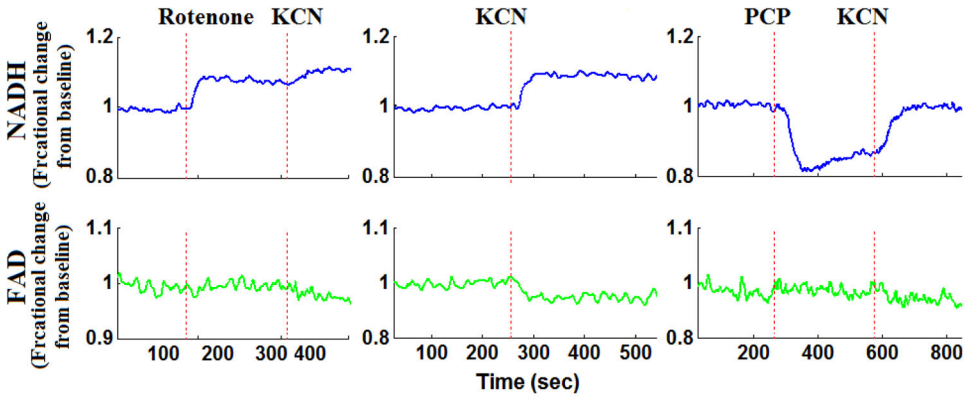

Fig. 5.

Representative fluorometer response to perfusion with chemical inhibitors and uncouplers in a hyperoxic lung.

Table I

The effects of metabolic inhibitors and uncoupler on the lung tissue surface FAD and NADH fluorescence signals of normoxic and hyperoxic rats.

Inhibitor/Uncoupler	FAD %		NADH %	
	Normoxic	Hyperoxic	Normoxic	Hyperoxic
Rotenone	0.2 ± 0.2	−0.3 ± 0.3	20.2 ± 2.3	7.5 ± 1.0 *
KCN	−6.8 ± 1.6	−5.2 ± 0.5	21.7 ± 2.5	9.2 ± 1.2 *
PCP	1.7 ± 0.8	−2.3 ± 1.4 *	−19.7 ± 2.1	−20.8 ± 1.2
PCP + KCN	−9.3 ± 1.0	−4.2 ± 0.7 *	25.7 ± 2.6	9.0 ± 1.0 *
Rotenone + KCN	−3.3 ± 0.8	−3.8 ± 0.6	4.6 ± 1.0	2.8 ± 1.2

Values are mean ± SE. For the (PCP + KCN) and (rotenone + KCN) treatments, the percentage change due to additional treatment with KCN is calculated relative to the new baseline in the presence of PCP or rotenone, respectively. For normoxic lungs, n = 5, 7, 6, 6, and 5 for rotenone, potassium cyanide (KCN), pentachlorophenol (PCP), PCP + KCN, and rotenone + KCN, respectively. For hyperoxic lungs, n = 4, 5, 6, 5, and 4 for rotenone, KCN, PCP, PCP + KCN, and rotenone + KCN, respectively.

* indicates value significantly different from the corresponding normoxic value (*t*-test, $P < 0.05$).

Table II

Mitochondrial complex I and complex II activity measured in P2 fractions of lung homogenate

	Complex I (nmol/min/mg protein)	Complex II (nmol/min/mg protein)
Normoxic	37.6 ± 3.2	79.1 ± 5.9
Hyperoxic	8.6 ± 0.7*	28.5 ± 2.3*

Values are mean ± SE. n = 4 and 3 for normoxic and hyperoxic lungs, respectively.

* indicates value significantly different from the corresponding normoxic value ($p < 0.05$; t-test).